Neural circuit basis of adolescent THC-induced potentiation of opioid responses later in life

Elizabeth Hubbard[1#], Vivienne Mae Galinato[1#], Pieter Derdeyn[2#], Katrina Bartas[2], Stephen V. Mahler[3], and Kevin T. Beier[1, 3-5*]

1 Department of Physiology and Biophysics, University of California, Irvine, Irvine, CA, USA 92697-4560

2 Program in Mathematical, Computational, and Systems Biology. University of California, Irvine, Irvine, CA, USA 92697-4560

3 Department of Neurobiology and Behavior, University of California, Irvine, Irvine, CA, USA 92697-4560

4 Department of Biomedical Engineering, University of California, Irvine, Irvine, CA, USA 92697-4560

5 Department of Pharmaceutical Sciences, University of California, Irvine, Irvine, CA, USA 92697-4560

Co-first authors

*Corresponding author

Contact information:

Kevin Beier

825 Health Sciences Road

Medical Sciences D337

Irvine, CA 92697

Phone: 949-824-1083

Email: kbeier@uci.edu

ABSTRACT:

Use of one drug of abuse typically influences the behavioral response to other drugs, either administered at the same time or a subsequent time point. The nature of the drugs being used, as well as the timing and dosing, also influence how these drugs interact. Here, we tested the effects of adolescent THC exposure on the development of morphine-induced behavioral adaptations following repeated morphine exposure during adulthood. We found that adolescent THC administration potentiated reward, and paradoxically impaired the development of morphine reward. Following a forced abstinence period, we then mapped the whole-brain response to a moderate dose of morphine, and found that adolescent THC administration led to increased morphine-induced activity in the basal ganglia and increased functional connectivity between frontal cortical regions and the ventral tegmental area. Last, we show using rabies virus-based circuit mapping that adolescent THC exposure triggers a long-lasting elevation in connectivity from the frontal cortex regions onto ventral tegmental dopamine cells. Our study adds to the rich literature on the interaction between drugs of abuse, including THC and opioids, and provides potential circuit substates by which adolescent THC exposure influences responses to morphine later in life.

INTRODUCTION:

Cannabis is currently the most widely used drug by adolescents in the United States[1]. Despite a reputation as a relatively harmless drug, over 30% of cannabis users meet the diagnostic criteria for cannabis use disorder (CUD)[2], a similar proportion to those who become addicted after trying “hard” drugs such as cocaine and opioids[3]. With the global trend toward cannabis legalization enabling increased access to cannabis, it is critical to understand how adolescent cannabis use impacts the brain and behavior, especially if it does so in a persistent manner in the dynamically developing adolescent brain. Adolescent exposure to the major psychoactive constituent of cannabis, tetrahydrocannabinol (THC), has been linked to a variety of negative outcomes later in life[4–6], including increased subsequent consumption of ‘harder” drugs[7–12]. Given the posited role of the mesolimbic dopamine system as the final common pathway for addiction[13], it is not surprising that brain regions such as the ventral tegmental area (VTA), medial prefrontal cortex (mPFC), and nucleus accumbens (NAc) are critically important in mediating the long-lasting effects of adolescent THC on responses to psychoactive drugs later in life[10,14–16]. Much like use of other psychoactive drugs[17–20], adolescent THC usage can lead to a hyperdopaminergic state[15] that then facilitates a variety of neuroadaptations that promote addiction. Despite this common framework, our mechanistic understanding of how adolescent THC causes persistent changes that linger until adulthood is limited.

Given that THC carries an addictive liability, it is critically important to understand the interactions between adolescent THC usage and exposure to drugs of abuse later in life, for example prescription opioids. It has long been hypothesized that cannabis use may predispose individuals to opioid use[21–23].

This is supported by the observation that cannabinoids and opioids may both activate the midbrain dopamine system, perhaps via common mechanisms of mu opioid receptor activation[24]. In addition, cross-sensitization of THC and morphine has been demonstrated[25], adolescent THC exposure can alter expression of genes related to the endogenous opioid system[10], as well as potentiate opioid-seeking behaviors later in life[26,27], providing further evidence that these drugs may work via common mechanisms. This is an important question because, despite the goal to reduce the clinical usage of opioids, opioids remain the primary treatment for post-operative pain management. In addition, approximately eighty percent of those who use heroin began using opioids for pain management[28,29]. Therefore, it is important to understanding mitigate the negative effects that adolescent THC may have on behavioral responses to opioids later in life.

Here, we administer a moderate dose of THC (5 mg/kg) for 14 days starting at postnatal day 30 (PD30), during adolescence. After a washout period during which mice develop to adulthood, we then test a variety of opioid-induced behaviors by administering morphine and assessing differential effects in those with or without a history of adolescent THC. After undergoing a forced abstinence period following repeated morphine injections, we also assess how adolescent THC administration influences brain-wide activity patterns following a moderate of morphine, as well as how adolescent THC administration alters connectivity onto dopamine neurons in the VTA.

METHODS:

All procedures were approved by the University of California, Irvine's Institutional Animal Care and Use Committee (IACUC) and carried out in accordance with the National Institutes of Health guidelines for the care and use of animals. Adolescent male and female C57BL/6J mice were weaned and sexed at PD21 and group housed with same-sex littermates. Mice were housed in standard individually ventilated cages with corncob bedding and two cotton nestlets for enrichment. Lights were on a 12 hr on/12 hr off cycle (7:30-7:30) and rooms have controlled temperature (22ºC +/- 2ºC) and humidity (55-65%). Mice received ad libitum access to food and water. Mice were housed in the Gillespie Neuroscience Research Facility (GNRF), except for during adolescent THC treatment. Mice were transferred to the McGaugh Hall mouse facility following weaning at approximately P25, and then returned to the GNRF at approximately P45.

<u>Adolescent THC Administration:</u> Mice were handled and weighed daily. On PD30, mice began daily injections of either 5 mg/kg THC or vehicle, which was prepared daily by dissolving in 5% Tween80 in saline. After 14 days of daily injections (PD30-PD43), mice were left in their home cage undisturbed (aside from weekly cage changes) until PD70 when behavioral testing began.

Drugs: THC was provided by the NIDA Drug Supply Program or Cayman Chemicals (Ann Arbor, MI) and administered at 5 mg/kg. Morphine was purchased from Patterson and was administered at 10 mg/kg.

Behavioral Testing:

Locomotion: The distance traveled in the open field was assessed during 30-minute recording sessions. Locomotion was assessed once per day for seven days, the first two following saline injections for habituation days, and the last five following injection of 10 mg/kg morphine.

Conditioned place preference: Custom two chamber acrylic boxes separated by a small corridor with distinct visual contexts on the walls of each side were used for CPP tests. On the pre-test day, mice were placed in the box with no barriers and were allowed to freely explore both sides for 30 minutes, and the time spent in each chamber was recorded. Following the pre-test, mice underwent two saline pairings and two morphine pairings. In the morning, the mice were given saline and paired with the preferred chamber, and in the afternoon, injected with morphine and paired with the non-preferred chamber. Control mice received saline in both contexts. On the post-test day, mice were again placed in the CPP chamber with no barriers, and the amount of time spent in each chamber was recorded. Data were plotted as the relative time spent on the drug-paired chamber in the post-test relative to the pre-test. Mice that spent over 1200 seconds on one side during the pre-test were excluded from analysis.

Elevated plus maze: Mice were placed at the end of one of the open arms, facing outwards. Mice were then able to freely explore the maze for 5 minutes, and the time spent in the open arms was recorded. Tests were performed in dim lighting ~25 lux.

Open field test: Mice were placed in a 40cm x 40cm square arena made of opaque plexiglass and were able to freely explore during a 5-minute test. During analysis, the arena was divided into nine equal square zones. The time spent in the center square for each mouse was calculated. Tests were performed under bright lighting conditions of ~1000 lux.

Marble burying: Mice were placed in a rat cage with 20 marbles placed on top of corn-cob bedding. After 30 minutes, the number of marbles that were buried by each mouse was recorded.

Von Frey: The von Frey test was used to assess mechanical sensitivity. Mice were placed on top of a wire mesh platform, restrained underneath a glass beaker, and allowed to acclimate for at least 30 minutes. The mouse's right hindpaw was gently touched with different filaments, starting with the 0.4g filament. If the mouse showed a withdrawal response (such as lifting, shaking, or licking the paw), the experimenter stepped down to a lighter filament, and if the mouse did not respond, the experimenter

131 stepped up to a thicker filament until a response occurred. The process continued with filaments of higher
132 or lower forces for four additional turns following the first change in response. This up/down method was
133 used to determine the mechanical force required to elicit a paw withdrawal response (50% threshold)[30].
134
135 cFos induction and immunohistochemistry: One hour following injection of 5 mg/kg morphine (a dose
136 used only for morphine-induced reinstatement), mice were perfused with PBS followed by 4%
137 formaldehyde, and brains isolated and post-fixed overnight in 4% formaldehyde. The following day, brain
138 clearing began using iDISCO[31]. The monoclonal rat anti-cFos antibody (Synaptic Systems lot #226017)
139 in 5% NDS/PBS-Tween 0.1% was used at a 1:5000 dilution, with an incubation time of five days. Donkey
140 anti-rat Cy3 (Jackson Immunoresearch) was then used at a dilution of 1:250. Brains were then cleared
141 in dibenzyl ether and imaged using a Zeiss Z1 light-sheet microscope. ClearMap[32] was then used to align
142 the imaged brains to the Allen Brain Reference Atlas, and to quantify the number of cFos+ neurons in
143 anatomically-defined brain regions.
144
145 Network Analysis: In order to relate functional connectivity using cFos labeling to anatomical connectivity,
146 anatomical projection data from the Allen Mouse Brain Connectivity Atlas was used to construct a
147 connectivity matrix among the brain regions in our analysis[33]. This atlas quantifies axonal arborization
148 from AAV injections to measure projections from one region to another. The density of each projection,
149 or the sum or projecting pixels divided by the total pixels in that region, was normalized by dividing by the
150 volume of injection, so as not to bias experiments with more virus injection than others. This quantity was
151 also multiplied by the number of voxels in the injection structure to avoid overrepresentation of smaller
152 regions. This quantity was computed for every pair of source and target regions to build a connectivity
153 matrix. We log-normalized these quantities so that they would have a more normal distribution and
154 behave better in network analysis. Community detection was performed using the Louvain algorithm with
155 a resolution parameter of 1, in the scit-kit network library[34]. Once the clusters were determined, the cFos
156 fold change of their regions were compared using a one-way ANOVA followed by pairwise t-tests.
157
158 Functional Analysis: Regional cFos counts across each mouse in the adolescent vehicle-treated and
159 THC-treated conditions were dimensionally reduced using UMAP, so that regions with similar counts
160 across the mice would be embedded close to each other[35]. Regions were clustered using HDBSCAN,
161 which can identify hierarchical clusters in continuous data based on variations in density of the data[36].
162 Hierarchical clustering was also performed on the correlations between regions, to look more closely at
163 their functional relationships. R^2 value from Pearson correlations were computed for each pair of regions,
164 based on their counts across mice of a given condition. Hierarchical clusterings were computed on
165 correlation matrices using the average linkages methodology. For visualizations, the hierarchical
166 clustering tree was cut at a height of 0.75 to determine the clusters (Figure 4I-J). The trees were cut for

167 heights between 0.5 and 1 to observe trends in modularity across the two conditions. The seaborn library
168 was used for all hierarchical clustering computations[37].
169
170 Rabies virus circuit mapping: Rabies virus (RABV) monosynaptic tracing studies were carried out as
171 previously described[19,38], with minor modifications. On Day 0, 100 nL of a 1:1 volume mixture of AAV-
172 CAG-FLEx^{loxP}-TC and AAV-CAG-FLEx^{loxP}-G was injected into the VTA of PD56 mice that had undergone
173 two weeks of THC injections between PD30 and PD43. Fourteen days later, RABV was injected into the
174 VTA. After recovery, mice were housed in a BSL2 facility for 5 days to allow RABV spread and GFP
175 expression. Mice were then perfused with PBS followed by 4% formaldehyde and postfixed overnight.
176 Fixed brains were cryoprotected by incubation in a 30% sucrose solution overnight, and frozen in OCT.
177 Brains were then serially sliced on a cryostat into 60 um sections. GFP+ cells throughout the brain in 22
178 anatomically-defined input sites were counted manually, as previously performed[19,38].
179
180 Viruses and injection coordinates: Coordinates used for the VTA were (relative to Bregma, midline, or
181 dorsal brain surface and in mm): AP − 3.20, ML 0.4, DV − 4.2.
182
183 The titers of viruses, based on quantitative PCR analysis, were as follows:
184 AAV-CAG-FLEx^{loxP}-TC, serotype 5, 2.4 x 10^{13} genome copies (gc)/ml
185 AAV-CAG-FLEx^{loxP}-G, serotype 8, 1.0 x 10^{12} gc/ml
186
187 For RABV, the titer was performed on HEK 293T-TVA800 cells.
188 RABV (EnvA-pseudotyped, GFP-expressing), 5.0 x 10^{8} colony forming units (cfu)/ml
189
190 After scaling RABV data, PCA was applied so features were brain regions and observations were
191 individual brains of mice treated with various drugs. Differences between mouse brains were
192 visualized by plotting PC1, PC2, and PC3 (Figure 5J-L, Q-R). Ellipsoids for each condition were
193 calculated and overlayed onto plots to visualize trends in PC values by condition. To further quantify
194 relationships between brains and conditions, the Euclidean distance between each point (or each
195 brain) in the PC1 versus PC2 coordinate space was calculated. These distances were then plotted
196 in a heatmap with brains being organized by similarity assessed by hierarchical clustering (Figure
197 5M). Alternatively, for a summary by condition, these distances were averaged based on drug
198 administered, and the resulting heatmap and clustering were made based on averaged Euclidean
199 distance values (Figure 5S). Heatmaps and clustering were made using the clustermap function in
200 the Python package seaborn with default parameters[37]. The RABV data that included single
201 injections of psychostimulants, morphine, or nicotine, or two anesthetic doses of ketamine/xylazine,

202 were presented in our published work[39] and used here for sake of comparison. For these
203 experiments, a single dose of 15 mg/kg cocaine, 1 mg/kg amphetamine, 2 mg/kg methamphetamine,
204 0.5 mg/kg nicotine, or 10 mg/kg morphine were given to adult mice, and RABV tracing was performed
205 the following day. These mice were anesthetized with isoflurane-based anesthesia, as used in this
206 manuscript. A separate group was anesthetized with a ketamine/xylazine mixture prior to both helper
207 virus injection and RABV injection, and not given another drug. RABV was introduced during the
208 second ketamine/xylazine injection.
209
210 Quantification and Statistical Analysis: Statistics for all studies were calculated using GraphPad Prism
211 9 software. Statistical significance between direct comparisons was assessed by unpaired or paired t-
212 tests. When multiple conditions were compared, one- or two-way ANOVAs were first performed, as
213 appropriate, then t-tests were then performed for each individual comparison. Multiple comparisons
214 corrections were performed when multiple such t-tests were being performed e.g., RABV input mapping
215 and cFos quantification, and significance was assessed using the Holm-Bonferroni method. In conditions
216 where multiple comparisons were performed and the results were still considered significant, asterisks
217 were presented corresponding to the original p-values. Paired t-tests were used in cases with repeat
218 measurements. Dot plots presented throughout the manuscript include a bar representing the mean value
219 for each group. Error bars represent s.e.m. throughout. For all figures, ns $P > 0.05$, * $P \leq 0.05$, ** $P \leq 0.01$,
220 *** $P \leq 0.001$, **** $P \leq 0.0001$.
221
222 **RESULTS:**
223 **Adolescent THC exposure history reduces morphine-induced locomotion, with no impact on**
224 **morphine reward**
225 We first exposed mice to a daily 5 mg/kg/day dose of THC (or its vehicle) during adolescence, here
226 defined as postnatal days 30-43 (Figure 1A). This is considered a moderate dose that is comparable to
227 doses self-administered by humans[40,41]. Following vehicle or THC administration, mice were left in their
228 home cages undisturbed besides weekly cage changes until postnatal day 70, at which time behavioral
229 testing commenced. The protocol of morphine administration and behavioral testing is shown in Figure
230 1B. To test how adolescent THC exposure history impacts morphine reward, we conducted a conditioned
231 place preference (CPP) test using 10 mg/kg morphine (Figure 1C). We induced a significant preference
232 to the morphine-paired side in both vehicle and THC exposed animals, to an approximately equivalent
233 extent. No preference was observed in animals treated with vehicle during adolescence and again at
234 adulthood in place of morphine (Vehicle/saline 762s pre, 778s post, $p = 0.22$; Vehicle/morphine 783s pre
235 vs. 887s post, $p = 0.038$; THC/morphine 785s pre vs. 887s post, $p = 0.0017$; Figure 1D). To determine
236 whether adolescent THC treatment impacted morphine-induced locomotion, we measured locomotor

behavior while mice were in an open field. Following a two-day habituation protocol where mice were given saline injections, 10 mg/kg morphine was given once per day for five days (Figure 1E) to test the sensitization or tolerance to morphine's effects on locomotion. We observed that morphine increased locomotion the most following the first dose, and this elevation was reduced with each subsequent dose, for both groups. We also found that that adolescent THC exposure overall blunted morphine-induced locomotion during the five-day morphine administration window (repeated measures Two-way ANOVA $p = 0.045$; Figure 1F), though no individual day was significantly different between the groups following multiple comparisons corrections. These data indicate that adolescent THC exposure reduced morphine-induced locomotion following morphine exposure later in life.

Adolescent THC exposure impairs the development of anxiety-related behavior and pain hypersensitivity during morphine withdrawal.

We next assessed whether mice treated with THC during adolescence were differentially impacted by withdrawal from repeated morphine administration. Following the five days of morphine given for locomotor testing and two days for CPP extinction, mice were left in their home cages for an additional 8 days, for a total abstinence period of ten days (Figure 2A). Following this ten-day forced abstinence, mice were tested for anxiety-like behavior using three tests: the elevated plus maze, open field test, and marble burying tests. The elevated plus maze tests how mice balance their tendency to explore against their preference for enclosed spaces (Figure 2B). A reduction in the time spent exploring the open arms is interpreted as anxiety-like behavior. Mice treated with repeated morphine injections spent less time in the open arms of the elevated plus maze relative to those treated with repeated saline injections. However, adolescent THC exposure blocked the reduction in time spent in the open arms induced by repeat morphine injection (One-way ANOVA $p = 0.0005$; pairwise t-tests, vehicle/saline vs. vehicle/morphine 47.73s vs. 17.84s, $p = 0.01$; vehicle/saline vs. THC/morphine 47.73s vs. 42.39s, $p = 0.67$; vehicle/morphine vs. THC/morphine 17.84s vs. 42.39s, $p = 0.0018$; Figure 2C). This suggests that adolescent THC exposure suppressed withdrawal-induced anxiety behaviors in response to adult opioid exposures. Similar results were observed using the open field test, where mice are both compelled to explore new environments, and avoid open areas (Figure 2D). Less time spent exploring the center of the arena is interpreted as anxiety-like behavior. We found that repeat morphine injections reduced time spent in the center of the open field, and THC history reduced this anxiety-like behavior (One-way ANOVA $p = 0.027$; pairwise t-tests, vehicle/saline vs. vehicle/morphine 22.66s vs. 12.55s, $p = 0.030$; vehicle/saline vs. THC/morphine 22.66s vs. 15.85s, $p = 0.077$; vehicle/morphine vs. THC/morphine 12.55s vs. 15.85s, $p = 0.59$; Figure 2E). Finally, in the marble burying test mice tend to bury marbles that are exposed in the bedding of a new cage (Figure 2F). In this assay, more marbles buried is interpreted to reflect increased anxiety-like behavior. We found that mice undergoing forced abstinence following repeat morphine injections buried more marbles after the 30-minute test, whereas adolescent THC

273 administration reduced this number, consistent with a reduced anxiety-like behavior (One-way ANOVA p
274 = 0.0006; pairwise t-tests, vehicle/saline vs. vehicle/morphine 0.93 vs. 3.67, p = 0.0048; vehicle/saline
275 vs. THC/morphine 0.93 vs. 0.50, p = 0.83; vehicle/morphine vs. THC/morphine 3.67 vs. 0.50, p = 0.006;
276 Figure 2G). Therefore, the results from each of these tests support the conclusion that adolescent THC
277 exposure decreases the expression of anxiety-like behaviors in morphine-treated mice.
278
279 Next, we used a von Frey assay to examine the effects of adolescent THC exposure on mechanical
280 hypersensitivity, both before and after morphine injection (Figure 2H). In addition to an increase in
281 anxiety-like behavior, mice undergoing physiological withdrawal following repeated opioid administration
282 show an increased pain sensitivity[42,43]. Mice treated with repeated THC doses during adolescence
283 showed no difference in mechanical thresholds when tested one day prior to morphine CPP testing
284 (Vehicle/morphine vs. THC/morphine 0.85g vs 0.86g, p = 0.93; Figure 2I). However, when tested again
285 following repeat morphine exposure and forced abstinence, mice given repeated morphine administration
286 showed an increased mechanical hypersensitivity relative to saline-treated controls, and adolescent THC
287 treated reduced the extent of this hypersensitivity (One-way ANOVA p = 0.0032; pairwise t-tests,
288 vehicle/saline vs. vehicle/morphine 1.09g vs. 0.42g, p = 0.0027; vehicle/saline vs. THC/morphine 1.09g
289 vs. 0.69g, p = 0.052; vehicle/morphine vs. THC/morphine 0.42g vs. 0.69g, p = 0.30; Figure 2J). Together,
290 these results indicate that adolescent THC exposure reduces the expression of morphine withdrawal-
291 induced behaviors following repeated morphine administration during adulthood.
292
293 **Adolescent THC exposure enhances drug-induced reinstatement of morphine CPP**
294 Following forced abstinence, we next assessed whether mice differentially reinstated CPP following a 5
295 mg/kg exposure of morphine in the CPP box. Drug exposure following abstinence can reinstate
296 previously extinguished drug-seeking behaviors, and therefore can serve as a model of relapse in mice.
297 Both groups of morphine-treated mice showed normal CPP (e.g., Figure 1D). Following CPP, mice then
298 underwent extinction. To reduce confounding factors while examining reinstatement, mice were excluded
299 that did not show CPP and proper extinction (N = 16 vehicle, 11 THC; Figure 3A-B). While mice treated
300 with vehicle during adolescence did not significantly reinstate CPP following the priming 5 mg/kg
301 morphine injection using this protocol, mice treated with THC during adolescence did significantly
302 reinstate their CPP (Vehicle/morphine-treated mice 722s vs 801.3s, = p = 0.43; THC/morphine treated
303 mice 780.7s vs. 1015s, p = 0.027; Figure 3C). This means that adolescent THC exposure drives
304 reinstatement of drug-seeking behavior in response to a sub-threshold dose of morphine in mice given
305 vehicle during adolescence.
306
307 **Whole-brain analysis shows differences in brain activity following drug-primed**
308 **reinstatement in adolescent vehicle- vs. THC-treated mice**

309 Given that adolescent THC-treated mice showed morphine-induced reinstatement whereas vehicle-
310 treated controls did not, we next assessed what neural pathways may be responsible for this effect. To
311 do this, we perfused the mice 60 minutes following the reinstatement test, cleared the brains using
312 iDISCO+, and immunostained for the immediately early gene cFos to obtain a brain-wide map of neuronal
313 activity (Figure 4A). We observed an overall elevation of neuronal activity in response to 5 mg/kg
314 morphine in mice treated with THC during adolescence than vehicle, as evidenced by a higher number
315 of cFos+ cells upon morphine exposure (Figure 4B). This increase was exhibited in most brain regions,
316 with some of the highest-fold elevations occurring in basal ganglia regions including the globus pallidus
317 externus (GPe), subthalamic nucleus (STN) and substantia nigra pars reticulata (SNr), as well as areas
318 such as the substantia innominate/ventral pallidum, and several thalamic regions (Figure 4B-D). In fact,
319 only four brain regions showed a reduction in cFos labeling in adolescent THC-treated mice, which
320 included both the medial and lateral habenula.
321
322 As the elevation in cFos labeling occurred globally in the mouse brain, we wanted to assess whether this
323 elevation was larger for some pathways or whether the activation was uniform. To test this, we built a
324 quantitative connectivity matrix of the mouse brain, using the Allen Mouse Brain Connectivity Atlas as a
325 template[33]. Doing so revealed the existence of four major network communities within the brain, largely
326 consisting of subcortical regions including the VTA (community 1, purple), cortical regions (community 2,
327 blue), the hippocampus and related connections (community 3, red), and mid/hindbrain regions
328 (community 4, yellow) (Figure 4E). We then assessed the relative increase in cFos labeling of regions in
329 each community in adolescent THC- vs. vehicle-treated mice following a reinstatement opioid dose. We
330 found a significant increase in the log fold-change cFos labeling in the purple and blue communities
331 relative to the yellow community, suggesting that the subcortical and cortical modules both showed an
332 overall larger increase in activity relative to mid/hindbrain regions in THC-treated mice (Figure 4F).
333
334 Following this analysis, we wanted to assess if these community-specific changes in cFos activation were
335 accompanied by any changes in the functional relationships of different brain regions. To do so, we took
336 the cFos labeling data across all regions for all mice and performed a dimensionality reduction analysis
337 using Uniform Manifold Approximation and Projection (UMAP). UMAP divided the brain regions into
338 approximately 10 activity-defined clusters in the adolescent THC-treated mice data. These clusters which
339 mapped relatively consistently onto the adolescent vehicle-treated mice data (Figure 4G-H), with a larger
340 distribution of brains from vehicle-treated compared to THC-treated mice. Interestingly, while frontal
341 cortex regions, including the mPFC subregions infralimbic cortex (IL), prelimbic cortex (PL), anterior
342 cingulate cortex (ACC), and anterior insula cortex (AI) all were in relatively close proximity in UMAP space
343 in both adolescent vehicle-treated mice and THC-treated mice, they clustered much more tightly together
344 in THC-treated group relative to the vehicle-treated group, indicating a higher level of correlated activity

following a reinstatement opioid exposure (Figure 4G-H). This suggests that adolescent THC exposure may increase the functional connectivity between frontal cortex regions and the VTA. To assess functional modularity more quantitatively, we built a brain-wide functional correlation matrix for adolescent THC-treated and vehicle-treated mice based on their cFos labeling (Figure 4I-J). While in vehicle-treated mice the VTA and frontal cortex regions separated into different clusters, reflecting their separation into different networks (Figure 4I), in THC-treated mice the IL, PL, ACC, and AI all co-clustered with the VTA, indicating a higher level of correlated activity amongst these regions in adolescent THC-treated mice (Figure 4J). Last, we wanted to assess the overall modularity of brain activity in adolescent THC- vs. vehicle-treated mice. To do this, we determined the number of unique clusters across a range of parameters. Across a wide parameter range, adolescent THC-treated mice exhibited fewer activity-defined clusters than vehicle-treated mice, reflecting an overall reduced modularity in brains from adolescent THC-treated mice (Figure 4K). These findings overall show that the increased activation of cortical and subcortical pathways in adolescent THC-treated vs vehicle-treated mice after reinstatement is accompanied by a collapse in modularity of pathways in adolescent THC-treated mice, including a tighter clustering of the VTA with frontal cortex regions.

Adolescent THC exposure changes connectivity to ventral tegmental area dopamine cells

VTA is a critical brain region for the development of a variety of drug-induced behavioral adaptations, including drug reward, sensitization, and withdrawal. To test whether adolescent THC exposure modified the input control to VTA dopamine (VTA^{DA}) cells, we mapped inputs to these cells using the rabies virus (RABV) monosynaptic input mapping method. First, in animals treated with THC during adolescence, Cre-dependent adeno-associated viruses (AAVs) expressing TVA and the RABV glycoprotein, RABV-G, were injected into the VTA of DAT-Cre mice. Two weeks later, mice were injected with a glycoprotein-deleted, EnvA-pseudotyped, GFP-expressing RABV (Figure 5A). This virus infected TVA-expressing cells by nature of the EnvA-TVA interaction. Once in VTA^{DA} cells, this virus could spread to their inputs, as RABV-G was expressed in DAT-Cre cells. However, once in input cells, since RABV did not express its own glycoprotein, the virus could not spread further. Five days later, experiments were terminated, and GFP-positive cells were counted throughout the brain as we did previously[19,39], and input connectivity was assessed. RABV-labeled input cells were observed throughout the brain, as in previous studies (Figure 5B-C)[19,39]. Overall, we observed several quantitative differences, shown in Figure 5D (Two-way ANOVA, interaction $p = 0.0062$). While several brain regions showed a visible difference in connectivity, for example elevated connectivity from cortical regions comprising the anterior cortex (infralimbic cortex, prelimbic cortex, anterior insula cortex, anterior cingulate cortex, and the anterior motor cortex[19,38,39,44]), parabrachial nucleus (PBN) and deep cerebellar nuclei (DCN), only the anterior cortex was significantly different following correction for multiple comparisons (corrected p-value $p = 0.029$).

381 This traditional approach to assessing differences in connectivity is statistically conservative, and only
382 assesses potential differences in connectivity, one input at a time. To reveal further patterns in the data,
383 we have recently employed a dimensionality reduction approach that enables us to detect larger-scale
384 differences in input patterns between brains of mice undergoing a variety of treatments[39,45]. We therefore
385 first used this approach to assess which inputs best differentiated THC-treated vs. control mice using
386 principal component analysis (PCA). We found that 3 PCs were sufficient to explain approximately 75%
387 of the variance in the data, and thus we focused only on these 3 PCs (Figure 5E-F). We found that PC1
388 completely separated THC-treated and control mice, whereas PC2 and PC3 did not (Figure 5G-I). Control
389 mice had high PC1 values, which were driven predominately by strong contributions from nucleus
390 accumbens medial shell (NAcMed), core (NAcCore), ventral pallidum (VP), septum, lateral habenula
391 (LHb) and medial habenula (MHb), while THC-treated mice had low PC1 values, which were driven by
392 the bed nucleus of the stria terminalis (BNST), extended amygdala area (EAM), entopeduncular nucleus
393 (EP), paraventricular nucleus of the hypothalamus (PVH), lateral hypothalamus (LH), and PBN (Figure
394 5G). To quantify these differences, we plotted each brain's location on each PC, and performed t-tests.
395 Differences between THC-treated and control groups were strongly significant along PC1, and not
396 different along PCs 2 and 3, as expected (Control 3.3 vs. THC -2.2, $p = 0.0002$). To further quantify
397 relationships between brains and conditions, the Euclidean distance between each brain in the PC1
398 versus PC2 coordinate space was calculated, and the relationships plotted as a correlogram. THC-
399 treated and control brains separated largely by condition, as expected (Figure 5M).
400
401 Last, we assessed how VTA^{DA} connectivity of THC-treated mice compares to mice treated with one of
402 several drugs, including a single dose of the psychoactive but non-addictive fluoxetine, two doses of the
403 anesthetic mixture of 100 mg/kg ketamine and 10 mg/kg xylazine, spaced 2 weeks apart, or one dose of
404 the addictive cocaine, amphetamine, methamphetamine, morphine, or nicotine, together grouped for
405 simplicity as "drugs of abuse". Using a similar PCA-based assessment, we observed that mice treated
406 with a drug of abuse separated from the other conditions along PC2, but not PC1 or PC3 (Figure 5N-P).
407 Interestingly, THC-treated mice had even higher values of PC2 than mice treated with one of the drugs
408 of abuse and were thus located further along PC2 from controls (Figure 5O-P). Positive values of PC2
409 were largely driven by strong contributions from the anterior cortex, BNST, EP, CeA, LH, PBN, and DCN,
410 notably many of the same regions that differentiated brains of THC-treated from controls (Figure 5G, N).
411 While PC3 did not strongly differentiate most of the groups, it did differentiate THC-treated mice from
412 those treated with a drug of abuse (Figure 5R). THC-treated mice had higher PC3 values, which were
413 driven by strong contributions from the anterior cortex, dorsal striatum (DStr), PVH, CeA, PBN, and DCN
414 (Figure 5N). The locations of each brain in PC space were plotted on bar graphs, and differences were
415 again assessed (PC2; Saline vs. THC -2.43 vs. 2.96, $p < 0.0001$; Fluoxetine vs. THC -1.55 vs. 2.96, $p =$
416 0.0004; K/X vs. THC -1.23 vs. 2.96 $p = 0.0024$; Drugs vs. THC 0.19 vs. 2.96, $p = 0.0051$. PC3; One-way

417 ANOVA p = 0.0004; Saline vs. THC 0.70 vs. 1.85, p = 0.63; Fluoxetine vs. THC 0.88 vs. 1.85, p = 0.71;
418 K/X vs. THC 0.19 vs. 1.85 p = 0.27; Drugs vs. THC -0.79 vs. 1.85, p = 0.0005; Figure 5Q-R). The distinct
419 connectivity patterns were also apparent following our Euclidean distance analysis in PC1 and PC2 space,
420 which indicated that the connectivity patterns from brains from THC-treated mice segregate completely
421 from those of mice treated with other psychoactive drugs (Figure 5S). Together, these results indicate
422 that adolescent THC treatment induces similar but distinct input changes onto VTA^{DA} neurons as previous
423 exposure to a single exposure to a "hard drug", principally an increase in connectivity from the anterior
424 cortex.
425
426 **DISCUSSION**:
427 Here, we tested the effects of adolescent THC exposure on later-life morphine-induced behaviors, brain-
428 wide activity following morphine reinstatement, and midbrain dopamine cell synaptic connectivity. We
429 found that adolescent THC exposure blunts morphine-induced locomotion and withdrawal anxiety/pain
430 hypersensitivity and enhances morphine-induced reinstatement following a forced abstinence period.
431 This broad range of effects is consistent with findings from studies that have explored the influence of
432 THC on morphine-induced behavioral changes[14,25–27,46]. Here, we extend these previous studies by
433 linking brain-wide activity patterns following a reinstatement dose of morphine to morphine-induced
434 reinstatement behavior and show that adolescent THC exposure creates long-lasting changes in input
435 connectivity to VTA^{DA} cells. Our study thus adds to a rich literature on the subject by implicating several
436 discrete circuits as potential drivers of the long-lasting effects of adolescent THC exposure on behavioral
437 and brain responses to opioids later in life.
438
439 It is perhaps surprising that THC exposure blunts morphine withdrawal-induced anxiety across several
440 behavioral assays, as well as pain sensitivity. Interestingly, the behavioral profile is consistent with the
441 behavioral responses observed following exposure of drugs of abuse during adolescence[47–51], where
442 adolescent mice experience potentiated drug reward with only mild withdrawal symptoms relative to adult
443 mice receiving equivalent drug exposures. This effect could be mediated by an occlusion of opioid-
444 induced epigenetic changes by those elicited following adolescent THC exposure. Such an effect was
445 previously observed following juvenile exposure to oxycodone; in this case, oxycodone induced long-
446 lasting epigenetic changes, for example an elevation of the repressive histone modification H3K27me3
447 on genes that control dopamine transmission in the VTA[52]. Therefore, one hypothesis is that adolescent
448 THC exposure may result in a similar imbalance of reward/aversion as is seen in responses to drugs
449 during adolescence by occluding compensatory responses to drug exposure that typically occur in
450 adulthood, but not adolescence. This could result, in, for example, withdrawal from repeated opioid
451 injection failing to induce a compensatory induction in anxiety-related behaviors and pain hypersensitivity.
452 In this case, reversal of these epigenetic marks may restore mice to basal levels of susceptibility. Future

453 studies are required to identify the potential cellular loci of these effects, as well as what the epigenetic
454 consequences of early life THC exposure may be.
455
456 In addition, we found that adolescent THC administration induces higher levels of drug-induced
457 reinstatement, consistent with previous observations assessing drug- or stress-induced
458 reinstatement[8,9,26]. Here, we extend these observations by linking these results to brain-wide cFos
459 activation in adolescent vehicle- vs. THC-treated mice. Overall, we found that adolescent THC-treated
460 mice had higher numbers of cFos+ cells in response to a 5 mg/kg reinstatement dose of morphine than
461 adolescent vehicle-treated controls. In addition, we found that adolescent THC-treated mice have higher
462 levels of correlated activity in mPFC and AI regions with the VTA than adolescent vehicle-treated mice,
463 indicating enhanced functional connectivity between these regions (Figure 4G-H). We previously showed
464 that activation of these cortical inputs to the VTA promotes reinforcement through increasing dopamine
465 release in the NAc[38]. Therefore, the elevated functional connectivity that we observe between these
466 regions in adolescent THC-treated mice may promote greater levels of dopamine release in the NAc than
467 in adolescent vehicle-treated mice and is one mechanism by which adolescent THC-treated mice may
468 more strongly reinstate morphine CPP following a priming dose of morphine.
469
470 However, one limitation of cFos-based analyses is that they do not consider anatomical connections.
471 Viral methods such as the monosynaptic RABV circuit mapping technique can specifically label
472 synaptically-connected cells[53,54]. Furthermore, we recently showed that the extent of input labeling is
473 dependent on the activity of input connections[19,20,55]. Therefore, our RABV mapping experiments have
474 the unique ability to explore the changes in connectivity to VTA^{DA} cells following repeated THC exposure,
475 without a preconceived bias as to which inputs may be altered. We have previously used this assay to
476 define how drugs of abuse change inputs to VTA^{DA} cells, enabling us to identify several pathway-specific
477 changes that have important consequences for the development of drug-induced behavioral
478 adaptations[39]. Here, we compare connectivity of VTA^{DA} cells in brains from mice receiving our adolescent
479 THC protocol to those receiving a single drug of abuse. We found that adolescent THC exposure induced
480 numerous long-lasting input changes onto VTA^{DA} cells that partially, but not completely, overlapped with
481 those induced by “hard drugs”. The most prominent difference between mice given adolescent THC
482 exposure vs. a drug of abuse is that THC-treated mice show a pronounced increase in inputs from the
483 anterior cortex (Figure 5D). Heightened activation of this connection is consistent with our cFos results
484 and would be expected to be rewarding through elevating activity in VTA^{DA} cells. This hypothesis is
485 consistent with the hyper-dopaminergic state of THC-treated animals previously reported[15], and the more
486 robust response in these animals to a reinstatement dose of morphine. In addition, we observed an
487 overall reduced modularity in adolescent THC-mice relative to adolescent vehicle-treated controls (Figure
488 4K). A reduction in brain modularity is seen following use and withdrawal from drugs of abuse[56–61] as well

489 as brain disorders such as traumatic brain injury and Alzheimer's-related dementia[62–67]. How this reduced
490 modularity may influence behavioral responses to drugs, however, remains largely unknown.
491
492 In our study, we also tested the hypothesis that adolescent THC exposure alters connectivity onto VTA
493 dopamine (VTA^{DA}) cells. This hypothesis was supported by the observation that rats treated with THC
494 during adolescence develop a hyper-dopaminergic state[15]; one potential mechanism that could mediate
495 this effect would be a change in connectivity to facilitate an increase in DA release in downstream brain
496 regions. Here, we found an elevation in inputs from the anterior cortex to VTA^{DA} cells, which we previously
497 showed promotes reinstatement by facilitating DA release in the NAc. Notably, we previously have shown
498 that a single injection of a variety of drugs of abuse can cause long-lasting changes in input connectivity
499 onto VTA^{DA} cells[19,20,55], with this signature being relatively similar regardless of the drug administered[19,39],
500 suggesting that these drugs induce similar changes in connectivity. The anterior cortex, particularly the
501 mPFC, is thought to play important roles in the later stages of substance use disorder[68–71]. The reduction
502 in connectivity from the anterior following a single dose, and increase in connectivity following repeated
503 doses, is thus consistent with that hypothesis of altered mPFC engagement during the addiction cycle.
504 One additional point of note is that we previously showed that drugs of abuse increase connectivity from
505 the globus pallidus externus (GPe) to the ventral midbrain, and that these changes are important for drug-
506 induced behavioral adaptations including reward and sensitization[19,20]. However, THC treatment did not
507 induce a notable change in GPe inputs onto VTA^{DA} cells (Figure 5D). Thus, while THC triggers several
508 long-lasting changes in connectivity to VTA^{DA} cells, these appear to be distinct from those initiated by
509 psychostimulants, nicotine, or morphine. However, the conclusions that we can draw from these
510 experiments are limited by differences in experimental design. For example, for the drug-treated mice,
511 RABV was injected one day following injection of the drug, whereas in THC-treated mice, they were
512 injected approximately 35 days following completion of a 2-week daily injection protocol. Thus, while in
513 the former study design drug-induced changes do not need to persist for longer than a few days to yield
514 the observed changes, in THC-treated animals the effects observed had to persist for longer than 35
515 days. In addition, THC was given fourteen times, once per day, whereas all other drugs were only given
516 once in total. Therefore, the effects observed with THC may result from repeated injections. However,
517 we performed the experiments presented here because our behavioral assessments were done 35 days
518 following completion of THC administration, and we wanted the RABV experiments to follow the same
519 timeline. Further experiments will be needed to resolve these questions.
520
521 **Acknowledgements:** We would like to thank Dr. Daniele Piomelli and the Impact of Cannabinoids
522 Across the Lifespan team at the University of California, Irvine for providing seed funding for this work.
523 This work was additionally funded by the NIH (R00 DA041445, DP2 AG067666, R01NS130044,
524 R01DA056599, 1R01DA054374), Tobacco Related Disease Research Program (T31KT1437,

525 T31P1426), One Mind (OM-5596678), Brightfocus Foundation (A2022031S), and the Brain and Behavior
526 Research Foundation (NARSAD 26845) to KTB, T32 GM136624 to KB and PD, NSF GRFP DGE-
527 1839285 to PD, T32DA050558 to EH, and R01DA055849, U01DA053826, R01MH132680, and
528 P50DA044118 to SVM.

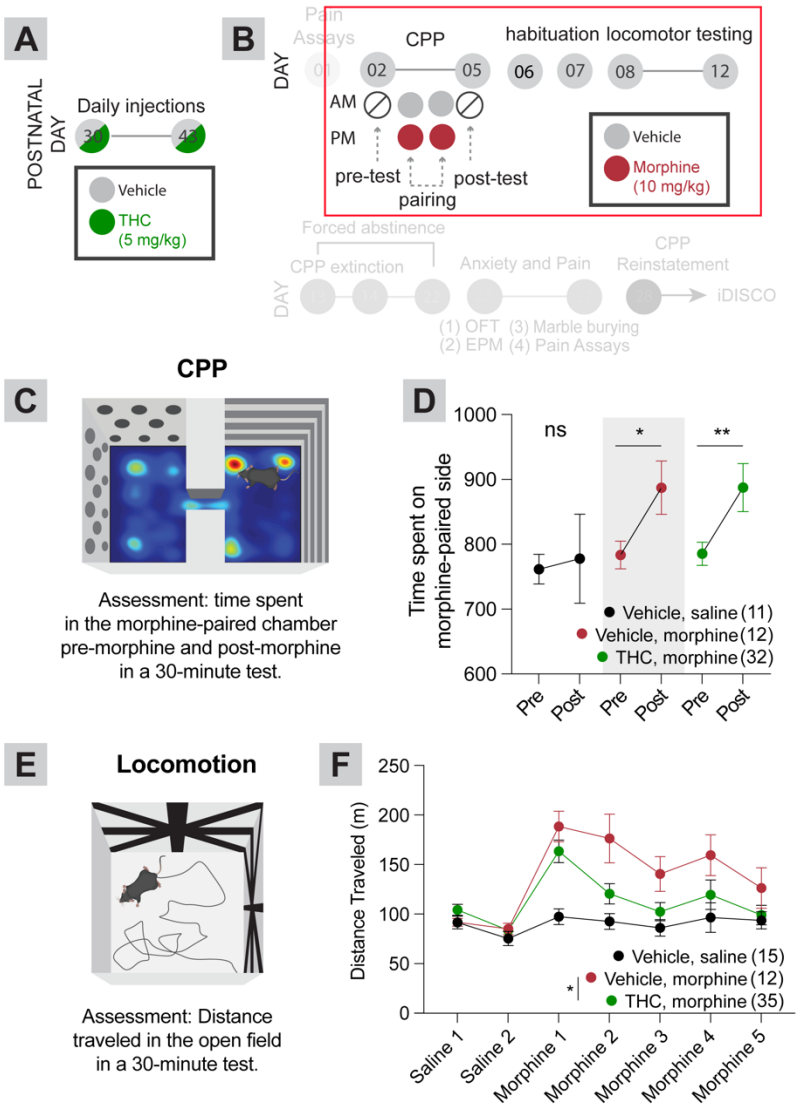

FIGURES:

Figure 1: Effects of adolescent THC exposure on behavioral responses to morphine administration later in life.

A, Timeline of THC or vehicle injections during adolescence. Injections were repeated once per day for 14 total days.

B, Morphine injections, and behavioral testing. The entire protocol is shown for each of Figures 1-3 for reference, with the relevant tests presented in the figure in full opacity and surrounded by red boxes.

C, Schematic of the conditioned place preference test.

D, Time spent in the morphine-paired chamber in the pre-test and post-test (in the vehicle/saline-paired group, both chambers were paired with saline). Vehicle/saline 762s pre, 778s post, $p = 0.22$; Vehicle/morphine 783s pre vs. 887s post, $p = 0.038$; THC/morphine 785s pre vs. 887s post, $p = 0.0017$.

E, Schematic of the locomotor test.

F, Mice treated with THC during adolescence showed an overall reduction in morphine-induced locomotion relative to mice treated with saline during adolescence. Repeat measures Two-way ANOVA between conditions $p = 0.045$; Sidak's multiple comparisons tests morphine day 1 $p = 0.68$, morphine day 2 $p = 0.24$, morphine day 3 $p = 0.31$, morphine day 4 $p = 0.50$, morphine day 5 $p = 0.75$. Vehicle/saline-treated mice are shown for comparison but were not included in statistical tests. Two-way ANOVA only included morphine injection days, not habituation days. For this and all figures, error bars = SEM, ns $p > 0.05$, * $p < 0.05$, ** $p < 0.01$, *** $p < 0.001$, **** $p < 0.0001$.

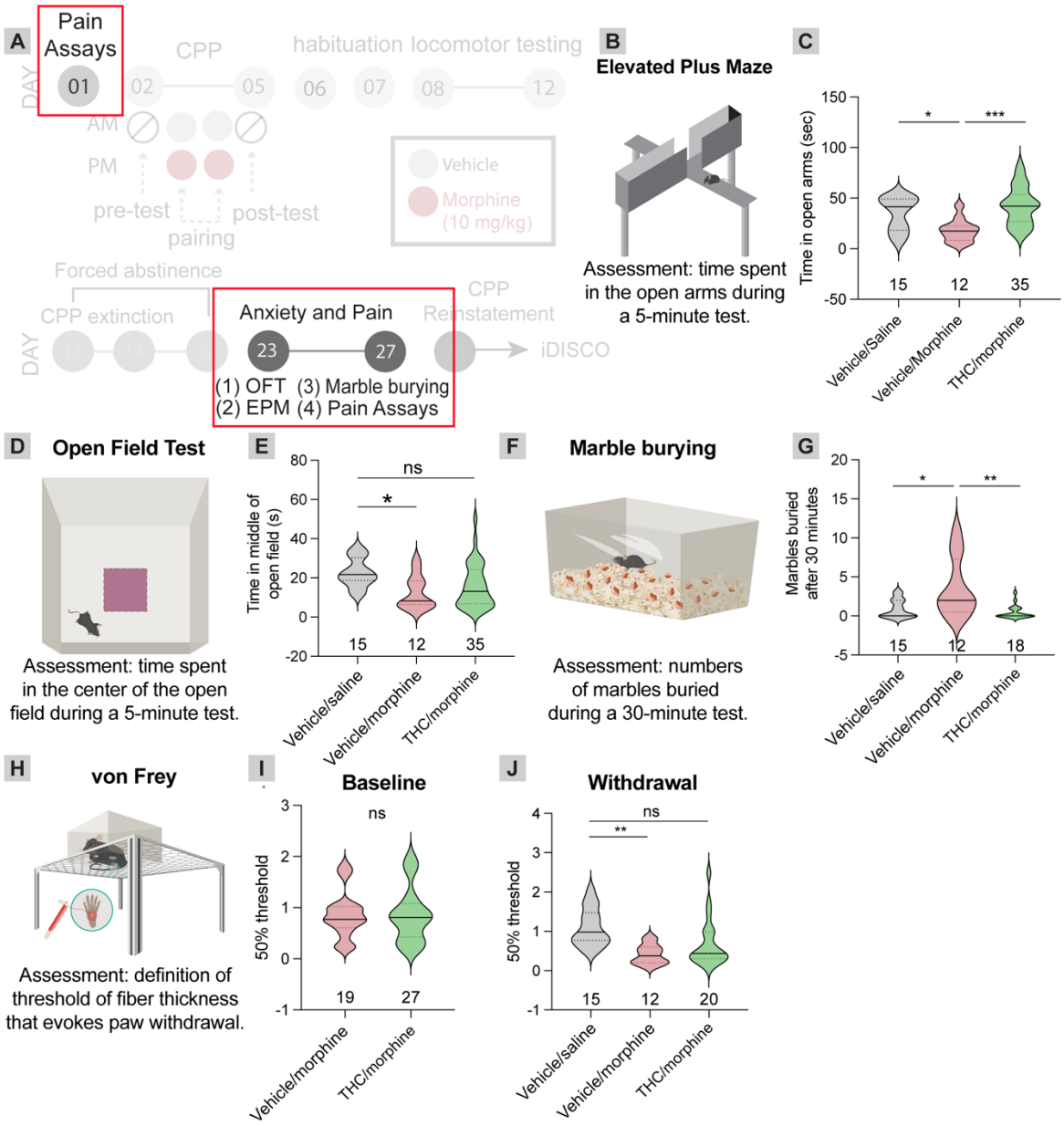

Figure 2: Adolescent THC administration reduces expression of morphine-induced withdrawal behaviors during a prolonged abstinence period.

A, Timeline of experiments.

B, Schematic of the elevated plus maze test.

C, Repeated morphine administration leads to a reduction in the time spent in the open arms of an elevated plus maze, indicative of anxiety-like behavior relative to mice treated with saline during adolescence, and saline during adulthood. Adolescent THC exposure prevented this morphine-induced anxiety. One-way ANOVA p = 0.0005; pairwise t-tests, vehicle/saline vs. vehicle/morphine 47.73 s vs. 17.84 s, p = 0.01; vehicle/saline vs. THC/morphine 47.73 s vs. 42.39 s, p = 0.67; vehicle/morphine vs. THC/morphine 17.84 s vs. 42.39 s, p = 0.0018.

D, Schematic of the open field test.

E, Repeated morphine administration leads to a reduction in the time spent in the center of an open field relative to mice treated with saline during adolescence, and saline during adulthood. Adolescent THC exposure blunted this reduction. One-way ANOVA $p = 0.027$; pairwise t-tests, vehicle/saline vs. vehicle/morphine 22.66 s vs. 12.55 s, $p = 0.030$; vehicle/saline vs. THC/morphine 22.66 s vs. 15.85 s, $p = 0.077$; vehicle/morphine vs. THC/morphine 12.55 s vs. 15.85 s, $p = 0.59$.

F, Schematic of the marble burying task.

G, Repeated morphine administration leads to an elevation in the number of marbles buried, indicative of anxiety-like behavior relative to mice treated with saline during adolescence, and saline during adulthood. Adolescent THC exposure prevented this morphine-induced anxiety. One-way ANOVA $p = 0.0006$; pairwise t-tests, vehicle/saline vs. vehicle/morphine 0.93 vs. 3.67, $p = 0.0048$; vehicle/saline vs. THC/morphine 0.93 vs. 0.50, $p = 0.83$; vehicle/morphine vs. THC/morphine 3.67 vs. 0.50, $p = 0.006$.

H, Schematic of the von Frey task of mechanical hypersensitivity.

I, Mice given saline vs. THC during adolescence showed no difference in baseline mechanical sensitivity. Vehicle/morphine vs. THC/morphine 0.85 g vs 0.86 g, $p = 0.93$. **J**, Repeated morphine administration leads to a reduction in the 50% mechanical threshold, indicative of pain hypersensitivity relative to mice treated with saline during adolescence, and saline during adulthood. Adolescent THC exposure blunted this morphine-induced pain hypersensitivity. One-way ANOVA $p = 0.0032$; pairwise t-tests, vehicle/saline vs. vehicle/morphine 1.09 vs. 0.42, $p = 0.0027$; vehicle/saline vs. THC/morphine 1.09 vs. 0.69, $p = 0.052$; vehicle/morphine vs. THC/morphine 0.42 vs. 0.69, $p = 0.30$.

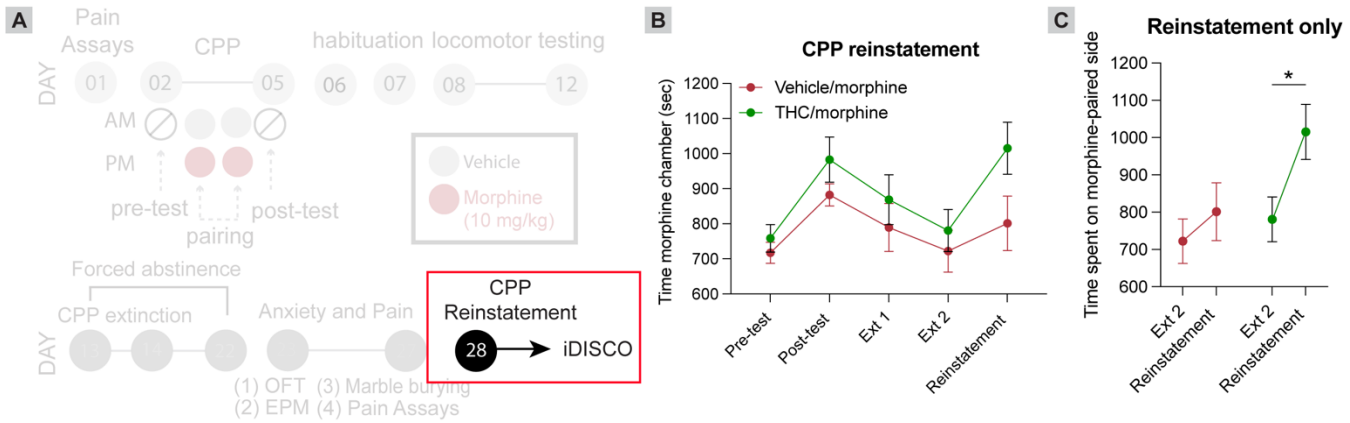

Figure 3: **Mice treated with THC during adolescence show an elevation in drug-induced reinstatement of morphine-seeking behaviors later in life**.

A, Timeline of experiments.

B, Time spent in the morphine-paired chamber during CPP pre-test, post-test, extinction, and reinstatement. Mice treated with THC or vehicle during adolescence showed a similar trajectory except for during reinstatement using a 5 mg/kg dose of morphine, at which time THC-treated mice showed an elevation in reinstatement behavior.

C, Quantification of the time spent in the morphine-paired chamber in the reinstatement task relative to the final extinction day. Vehicle/morphine-treated mice 722 s vs 801.3 s, $p = 0.43$, $n = 12$ each; THC/morphine treated mice 780.7 s vs. 1015 s, $p = 0.027$, $n = 8$ each.

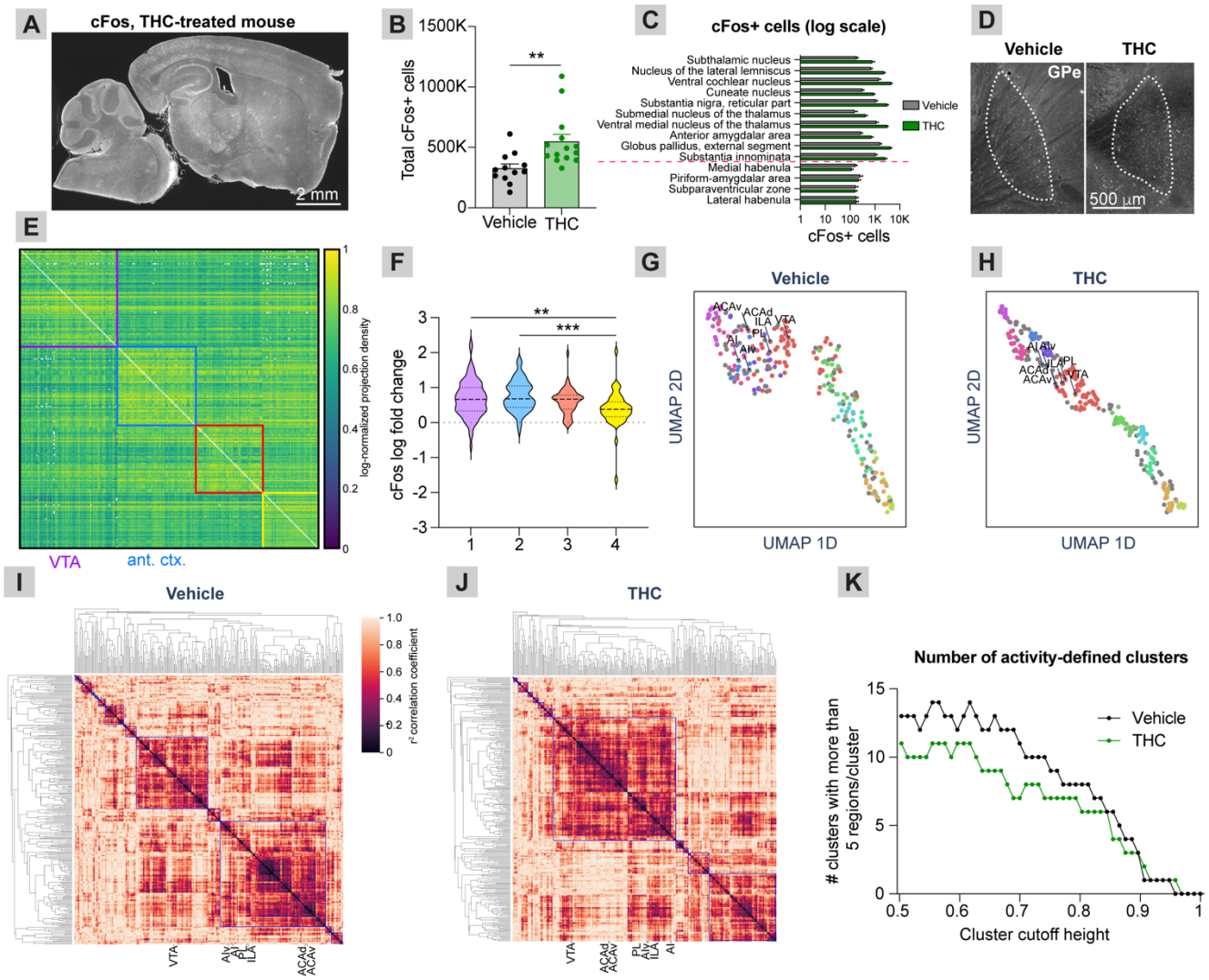

Figure 4: Brain-wide activity patterns in adolescent vehicle- and THC-treated mice following a reinstatement dose of morphine.

A, Representative sagittal section of a cFos-stained brain of an animal treated with THC during adolescence and following a reinstatement dose of morphine. Scale, 2 mm.

B, More cFos-expressing cells were detected in adolescent THC-treated mice than vehicle-treated mice following a dose of 5 mg/kg morphine (548,481 vs. 325,789 cells, $p = 0.0051$).

C, The top ten brain regions showing the highest-fold elevation in cFos labeling in adolescent THC-treated relative to vehicle-treated mice and the four regions showing an elevation in vehicle-treated mice. Groups are separated by the dashed red line. Shown are brain regions with an average > 150 cFos+ cells in each brain region.

D, Representative sagittal images of the GPe in adolescent vehicle-treated vs. THC-treated mice. Scale, 500 µm.

E, Anatomical connectivity matrix of the mouse brain, broken into four communities based on the Louvain method for community detection

606 **F**, Log fold-change in cFos labeling in each network community relative to one another (One-way ANOVA
607 p = 0.0002; purple (1) vs. blue (2) 0.68 vs. 0.75, p = 0.76; purple (1) vs. red (3) 0.68 vs. 0.61, p = 0.82;
608 purple (1) vs. yellow (4) 0.68 vs. 0.38, p = 0.0024; blue (2) vs. red (3) 0.75 vs. 0.61, p = 0.31; blue (2)
609 vs. yellow (4) 0.68 vs. 0.38, p = 0.0002; red (3) vs. yellow (4) 0.61 vs. 0.38, p = 0.05.
610 **G**, UMAP embedding of regions based on their correlated activity in adolescent vehicle-treated mice.
611 Each point is a brain region.
612 **H**, UMAP embedding of regions based on their correlated brain activity in adolescent THC-treated mice.
613 The regions are overall more tightly clustered than in panel G, suggesting a greater level of correlated
614 activity in adolescent THC-treated mice.
615 **I**, Hierarchical clustering of regions based on the cFos correlation matrix in adolescent vehicle-treated
616 mice. The VTA is within a separate activity-defined cluster from the frontal cortex regions of interest
617 (prelimbic cortex, PL; infralimbic cortex, ILA; anterior insula cortex, AI; anterior insula cortex, ventral part,
618 AIv; ACAd, anterior cingulate cortex, dorsal part; ACAv, anterior cingulate cortex, ventral part).
619 **J**, Hierarchical clustering of regions based on the cFos correlation matrix in adolescent THC-treated mice.
620 The VTA co-clusters with regions of the anterior cortex in these mice.
621 **K**, The number of hierarchical clusters in adolescent vehicle-treated and THC-treated mice across a
622 range of heights for cluster cut-offs in hierarchical trees. The THC-treated mice show reduced modularity
623 across a range of cutoff values.

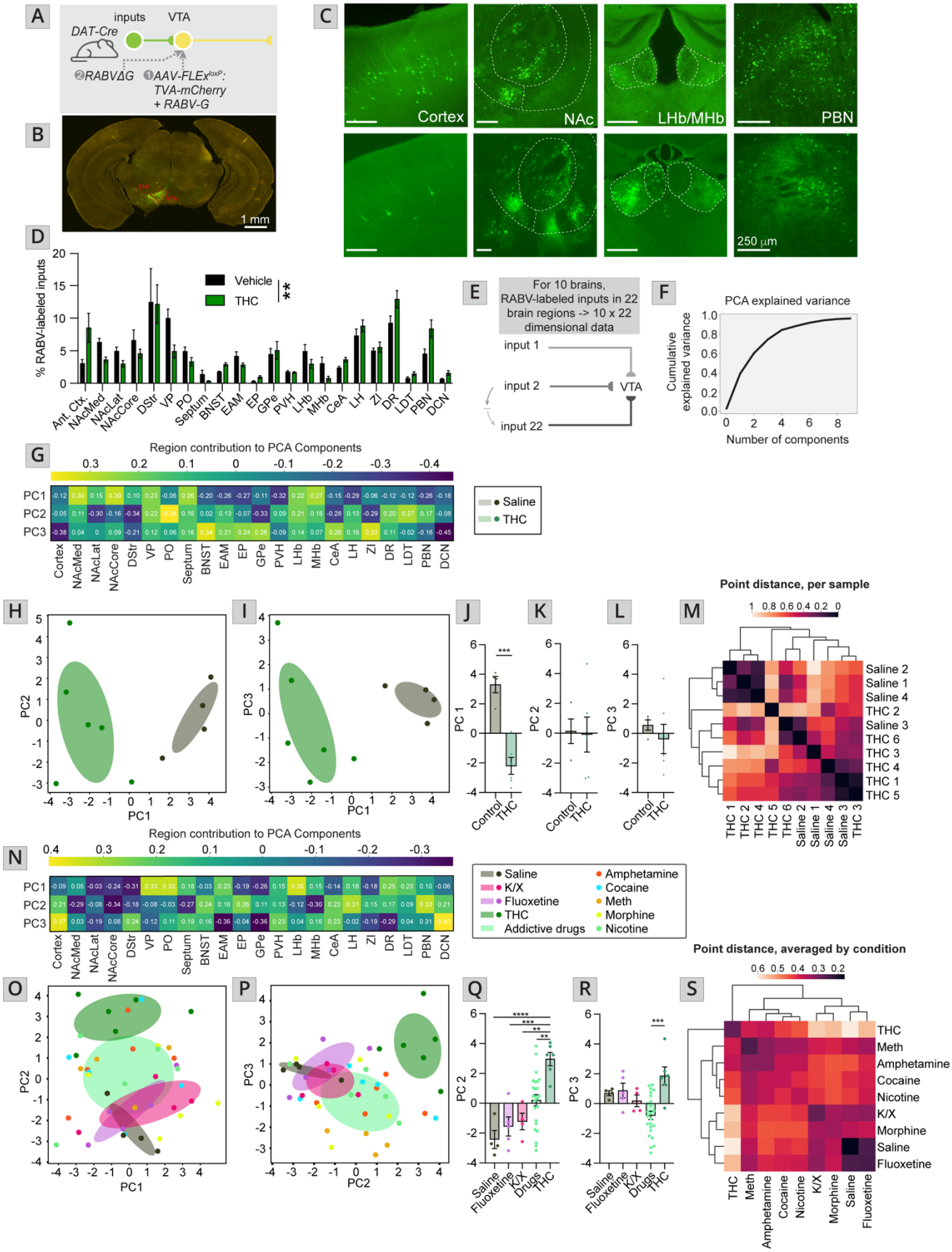

Figure 5: THC-treated mice show a different brain-wide pattern relative to animals treated with psychostimulants, opioids, or nicotine.

A, Schematic of experiments.

B, Representative image of the ventral midbrain of a DAT-Cre mouse showing starter cells in the VTA and medial SNc. Scale, 1 mm.

C, Representative images of input cell populations in several brain sites, including the anterior cortex, NAcMed, NAcCore, NAcLat, MHb, LHb, and PBN. Scale, 250 μm.

D, Bar graph plot showing the percentage of RABV-labeled inputs in control vs. THC-treated mice. Two-way ANOVA, interaction $p = 0.0062$. Only the anterior cortex was significantly different following correction for multiple comparisons (corrected p-value $p = 0.029$.

E, Schematic and explanation for how PCA analysis was carried out on the RABV tracing dataset.

F, Percent of cumulative variance explained by each principal component.

G, Heatmap of the contributions of each brain region, or feature, in the data to PCs 1 through 3.

H, Plot of PC1 and PC2 from brains of control and THC-treated mice.

I, Plot of PC1 and PC3 from brains of control and THC-treated mice.

J-L, Comparison of total PC values for each brain along **J** PC 1, **K** PC 2, and **L** PC 3. **J**, Control 3.3 vs. THC -2.2, $p = 0.0002$. **K**, Control 0.13 vs. THC -0.09, $p = 0.89$. **L**, Control 0.57 vs. THC -0.38, $p = 0.48$.

M, To further quantify relationships between brains and conditions, the Euclidean distance between each brain from control and THC-treated mice in the PC1 versus PC2 (or PC1 vs. PC3) coordinate space was calculated. These distances were then plotted in a heatmap with brains being organized by similarity assessed by hierarchical clustering.

N, Heatmap of the contributions of each brain region, or feature, in the data to PCs 1 through 3 in the data presented in panels N-Q.

O, Plot of PC1 and PC2 from brains of control and drug-treated mice.

P, Plot of PC1 and PC3 from brains of control and drug-treated mice.

Q-R, Comparison of total PC values for each brain along **Q** PC 2, and **R** PC 3. For PC 1, One-way ANOVA $p = 0.83$. **Q**, One-way ANOVA $p < 0.0001$; pairwise t-tests and asterisks presented in the figure include THC comparisons only, although statistics are based on comparisons between all groups. Saline vs. THC -2.43 vs. 2.96, $p < 0.0001$; Fluoxetine vs. THC -1.55 vs. 2.96, $p = 0.0004$; K/X vs. THC -1.23 vs. 2.96 $p = 0.0024$; Drugs vs. THC 0.19 vs. 2.96, $p = 0.0051$. **R**, One-way ANOVA $p = 0.0004$; Saline vs. THC 0.70 vs. 1.85, $p = 0.63$; Fluoxetine vs. THC 0.88 vs. 1.85, $p = 0.71$; K/X vs. THC 0.19 vs. 1.85 $p = 0.27$; Drugs vs. THC -0.79 vs. 1.85, $p = 0.0005$.

S, The Euclidean distance between each psychoactive drug-treated and control brain in the PC1 versus PC2 coordinate space was calculated, plotted in a heatmap, and brains were organized by similarity and assessed by hierarchical clustering.

REFERENCES:

1. National Center for Drug Abuse Statistics. Drug Abuse Statistics. (2024).

2. Hasin, D. S. *et al.* Prevalence of marijuana use disorders in the United States between 2001-2002 and 2012-2013. *JAMA Psychiatry* vol. 72 1235–1242 Preprint at https://doi.org/10.1001/jamapsychiatry.2015.1858 (2015).

3. Ferland, J. M. N. & Hurd, Y. L. Deconstructing the neurobiology of cannabis use disorder. *Nat Neurosci* **23**, 600–610 (2020).

4. Ruiz, C. M. *et al.* Pharmacokinetic, behavioral, and brain activity effects of ?9-tetrahydrocannabinol in adolescent male and female rats. *Neuropsychopharmacology* **46**, 959–969 (2021).

5. Chadwick, B., Miller, M. L. & Hurd, Y. L. Cannabis Use during Adolescent Development: Susceptibility to Psychiatric Illness. *Front Psychiatry* **4**, (2013).

6. Rubino, T., Zamberletti, E. & Parolaro, D. Adolescent exposure to cannabis as a risk factor for psychiatric disorders. *Journal of Psychopharmacology* vol. 26 177–188 Preprint at https://doi.org/10.1177/0269881111405362 (2012).

7. Panlilio, L. V., Zanettini, C., Barnes, C., Solinas, M. & Goldberg, S. R. Prior exposure to THC increases the addictive effects of nicotine in rats. *Neuropsychopharmacology* **38**, 1198–1208 (2013).

8. Stopponi, S. *et al.* Chronic THC during adolescence increases the vulnerability to stress-induced relapse to heroin seeking in adult rats. *European Neuropsychopharmacology* **24**, 1037–1045 (2014).

9. Lecca, D. *et al.* Adolescent cannabis exposure increases heroin reinforcement in rats genetically vulnerable to addiction. *Neuropharmacology* **166**, (2020).

10. Ellgren, M., Spano, S. M. & Hurd, Y. L. Adolescent cannabis exposure alters opiate intake and opioid limbic neuronal populations in adult rats. *Neuropsychopharmacology* **32**, 607–615 (2007).

11. Panlilio, L. V., Solinas, M., Matthews, S. A. & Goldberg, S. R. Previous exposure to THC alters the reinforcing efficacy and anxiety-related effects of cocaine in rats. *Neuropsychopharmacology* **32**, 646–657 (2007).

12. Friedman, A. L., Meurice, C. & Jutkiewicz, E. M. Effects of adolescent Δ9-tetrahydrocannabinol exposure on the behavioral effects of cocaine in adult Sprague–Dawley rats. *Exp Clin Psychopharmacol* **27**, 326–337 (2019).

13. Lüscher, C. & Malenka, R. C. Drug-Evoked Synaptic Plasticity in Addiction: From Molecular Changes to Circuit Remodeling. *Neuron* **69**, 650–663 (2011).

14. Rubino, T. *et al.* The Depressive Phenotype Induced in Adult Female Rats by Adolescent Exposure to THC is Associated with Cognitive Impairment and Altered Neuroplasticity in the Prefrontal Cortex. *Neurotox Res* **15**, 291–302 (2009).

15. Renard, J. *et al.* Adolescent Cannabinoid Exposure Induces a Persistent Sub-Cortical Hyper-Dopaminergic State and Associated Molecular Adaptations in the Prefrontal Cortex. *Cereb Cortex* **27**, 1297–1310 (2017).

16. Renard, J. *et al.* Adolescent THC Exposure Causes Enduring Prefrontal Cortical Disruption of GABAergic Inhibition and Dysregulation of Sub-Cortical Dopamine Function /631/378/2571 /631/378/1689/1799 /9 /9/30 /82 /82/1 article. *Sci Rep* **7**, (2017).

17. Creed, M. *et al.* Cocaine exposure enhances the activity of ventral tegmental area dopamine neurons via calcium-impermeable NMDARs. *Journal of Neuroscience* **36**, 10759–10768 (2016).

18. Bocklisch, C. *et al.* Cocaine Disinhibits Dopamine Neurons by Potentiation of GABA Transmission in the Ventral Tegmental Area. *Science (1979)* **341**, 1521–1525 (2013).

19. Beier, K. T. *et al.* Rabies screen reveals GPe control of cocaine-triggered plasticity. *Nature* **549**, 345–350 (2017).

20. Tian, G. *et al.* Molecular and circuit determinants in the globus pallidus mediating control of cocaine-induced behavioral plasticity. *Neuron Sneak Peek* (2023).

21. Kandel, D. B. Marijuana Users in Young Adulthood. *Arch Gen Psychiatry* **41**, 200–209 (1984).

22. Clayton, R. & Voss, H. Young men and drugs in Manhattan: a causal analysis. *NIDA Res. Monogr.* **39**, 1–187 (1981).

23. O'Donnell, J. & Clayton, R. The stepping-stone hypothesis--marijuana, heroin, and causality. *Chem Depend.* **4**, 229–241 (1982).

24. Tanda, G., Pontieri, F. E. & Chiara, G. Di. *Cannabinoid and Heroin Activation of Mesolimbic Dopamine Transmission by a Common 1 Opioid Receptor Mechanism*. https://www.science.org.

25. Cadoni, C., Valentini, V. & Di Chiara, G. Behavioral sensitization to Δ9-tetrahydrocannabinol and cross-sensitization with morphine: Differential changes in accumbal shell and core dopamine transmission. *J Neurochem* **106**, 1586–1593 (2008).

26. Ellgren, M., Spano, S. M. & Hurd, Y. L. Adolescent cannabis exposure alters opiate intake and opioid limbic neuronal populations in adult rats. *Neuropsychopharmacology* **32**, 607–615 (2007).

27. Tomasiewicz, H. C. *et al.* Proenkephalin mediates the enduring effects of adolescent cannabis exposure associated with adult opiate vulnerability. *Biol Psychiatry* **72**, 803–810 (2012).

28. Cicero, T. J., Ellis, M. S., Surratt, H. L. & Kurtz, S. P. The changing face of heroin use in the United States a retrospective analysis of the past 50 years. *JAMA Psychiatry* **71**, 821–826 (2014).

29. Muhuri, P., Gfroerer, J. & Davies, M. *Substance Abuse and Mental Health Services Administration. Associations of Nonmedical Pain Reliever Use and Initiation of Heroin Use in the United States*. (2013).

30. Chaplan, S. R., Bach, F. W., Pogrel, J. W., Chung, J. M. & Yaksh, T. L. Quantitative assessment of tactile allodynia in the rat paw. *J Neurosci Methods* **53**, 55–63 (1994).

31. Renier, N. *et al.* IDISCO: A simple, rapid method to immunolabel large tissue samples for volume imaging. *Cell* **159**, 896–910 (2014).

32. Renier, N. *et al.* Mapping of Brain Activity by Automated Volume Analysis of Immediate Early Genes. *Cell* **165**, 1789–1802 (2016).

33. Oh, S. W. *et al.* A mesoscale connectome of the mouse brain. *Nature* **508**, 207–214 (2014).

735 34. Muller, B., Richards, A. J., Jin, B. & Lu, X. GOGrapher: A Python library for GO graph
736 representation and analysis. *BMC Res Notes* **2**, (2009).

737 35. McInnes, L., Healy, J. & Melville, J. UMAP: Uniform Manifold Approximation and Projection for
738 Dimension Reduction. *ArXiv* **1802.03426**, 1–51 (2018).

739 36. McInnes, L., Healy, J. & Astels, S. hdbscan: Hierarchical density based clustering. *The Journal of*
740 *Open Source Software* **2**, 205 (2017).

741 37. Waskom, M. Seaborn: Statistical Data Visualization. *J Open Source Softw* **6**, 3021 (2021).

742 38. Beier, K. T. *et al.* Circuit Architecture of VTA Dopamine Neurons Revealed by Systematic Input-
743 Output Mapping. *Cell* **162**, 622–634 (2015).

744 39. Bartas, K. *et al.* Drug-induced changes in connectivity to midbrain dopamine cells revealed by
745 rabies monosynaptic tracing. *Elife* **13**, RP93664 (2024).

746 40. Cooper, Z. D. & Haney, M. Comparison of subjective, pharmacokinetic, and physiological effects
747 of marijuana smoked as joints and blunts. *Drug Alcohol Depend* **103**, 107–113 (2009).

748 41. Huestis, M. A., Henningfield, J. E. & Cone, E. J. Blood Cannabinoids. I. Absorption of THC and
749 Formation of 11-OH-THC and THCCOOH During and After Smoking Marijuana*. *J Anal Toxicol* **16**,
750 276–282 (1992).

751 42. Koob, G. F. Neurobiology of Opioid Addiction: Opponent Process, Hyperkatifeia, and Negative
752 Reinforcement. *Biol Psychiatry* **87**, 44–53 (2020).

753 43. Koob, G. F. Drug addiction: Hyperkatifeia/negative reinforcement as a framework for medications
754 development. *Pharmacol Rev* **73**, 163–201 (2021).

755 44. Beier, K. T. *et al.* Topological Organization of Ventral Tegmental Area Connectivity Revealed by
756 Viral-Genetic Dissection of Input-Output Relations. *Cell Rep* **26**, 159-167.e6 (2019).

757 45. Derdeyn, P., Hui, M., Macchia, D. & Beier, K. Uncovering the Connectivity Logic of the Ventral
758 Tegmental Area. *Front Neural Circuits* **15**, 799688 (2022).

759 46. Cadoni, C., Pisanu, A., Solinas, M., Acquas, E. & Di Chiara, G. Behavioural sensitization after
760 repeated exposure to Δ9-tetrahydrocannabinol and cross-sensitization with morphine.
761 *Psychopharmacology (Berl)* **158**, 259–266 (2001).

762 47. Levin, E. D., Rezvani, A. H., Montoya, D., Rose, J. E. & Scott Swartzwelder, H. Adolescent-onset
763 nicotine self-administration modeled in female rats. *Psychopharmacology (Berl)* **169**, 141–149
764 (2003).

765 48. Faraday, M. M., Elliott, B. M. & Grunberg, N. E. *Adult vs. Adolescent Rats Differ in Biobehavioral*
766 *Responses to Chronic Nicotine Administration*. www.elsevier.com/locate/pharmbiochembeh.

767 49. Vastola, B. J., Douglas, L. A., Varlinskaya, E. I. & Spear, L. P. *Nicotine-Induced Conditioned Place*
768 *Preference in Adolescent and Adult Rats*.

769 50. Faraday MM, Elliott BM, Phillips JM & Grunberg NE. Adolescent and adult male rats differ in
770 sensitivity to nicotine's activity effects. *Pharmacol Biochem Behav.* **74**, 917–931 (2003).

51. O'Dell, L. E., Bruijnzeel, A. W., Ghozland, S., Markou, A. & Koob, G. F. Nicotine withdrawal in adolescent and adult rats. in *Annals of the New York Academy of Sciences* vol. 1021 167–174 (New York Academy of Sciences, 2004).

52. Carpenter, M. D., Manners, M. T., Heller, E. A. & Blendy, J. A. Adolescent oxycodone exposure inhibits withdrawal-induced expression of genes associated with the dopamine transmission. *Addiction Biology* **26**, (2021).

53. Wickersham, I. R. *et al.* Monosynaptic Restriction of Transsynaptic Tracing from Single, Genetically Targeted Neurons. *Neuron* **53**, 639–647 (2007).

54. Wall, N. R., Wickersham, I. R., Cetin, A., De La Parra, M. & Callaway, E. M. Monosynaptic circuit tracing in vivo through Cre-dependent targeting and complementation of modified rabies virus. *Proc Natl Acad Sci U S A* **107**, 21848–21853 (2010).

55. Tian, G. *et al.* An extended Amygdala-midbrain circuit controlling cocaine withdrawal-induced anxiety and reinstatement. *Cell Rep* **39**, 1–16 (2022).

56. Kimbrough, A. *et al.* Brain-wide functional architecture remodeling by alcohol dependence and abstinence. *PNAS* **117**, 2149–2159 (2020).

57. Orsini, C. A., Colon-Perez, L. M., Heshmati, S. C., Setlow, B. & Febo, M. Functional connectivity of chronic cocaine use reveals progressive neuroadaptations in neocortical, striatal, and limbic networks. *eNeuro* **5**, (2018).

58. Konova, A. B., Moeller, S. J., Tomasi, D. & Goldstein, R. Z. Effects of chronic and acute stimulants on brain functional connectivity hubs. *Brain Res* **1628**, 147–156 (2015).

59. Liang, X. *et al.* Interactions between the salience and default-mode networks are disrupted in cocaine addiction. *Journal of Neuroscience* **35**, 8081–8090 (2015).

60. Tomasi, D. *et al.* Disrupted functional connectivity with dopaminergic midbrain in cocaine abusers. *PLoS One* **5**, (2010).

61. Konova, A. B., Moeller, S. J., Tomasi, D., Volkow, N. D. & Goldstein, R. Z. Effects of methylphenidate on resting-state functional connectivity of the mesocorticolimbic dopamine pathways in cocaine addiction. *JAMA Psychiatry* **70**, 857–868 (2013).

62. Bertolero, M. A., Yeo, B. T. T., Bassett, D. S. & D'Esposito, M. A mechanistic model of connector hubs, modularity and cognition. *Nat Hum Behav* **2**, 765–777 (2018).

63. Gallen, C. L. *et al.* Modular brain network organization predicts response to cognitive training in older adults. *PLoS One* **11**, (2016).

64. Brier, M. R. *et al.* Functional connectivity and graph theory in preclinical Alzheimer's disease. *Neurobiol Aging* **35**, 757–768 (2014).

65. De Haan, W. *et al.* Disrupted modular brain dynamics reflect cognitive dysfunction in Alzheimer's disease. *Neuroimage* **59**, 3085–3093 (2012).

66. Arnemann, K. L. *et al. Functional Brain Network Modularity Predicts Response to Cognitive Training after Brain Injury*. https://www.neurology.org (2015).

67. Sporns, O. & Betzel, R. F. Modular brain networks. *Annu Rev Psychol* **67**, 613–640 (2016).

68. Koob, G. F. & Volkow, N. D. Neurocircuitry of addiction. *Neuropsychopharmacology* **35**, 217–238 (2010).

69. Goldstein, R. Z. & Volkow, N. D. Dysfunction of the prefrontal cortex in addiction: Neuroimaging findings and clinical implications. *Nat Rev Neurosci* **12**, 652–669 (2011).

70. Volkow, N. D., Michaelides, M. & Baler, R. The neuroscience of drug reward and addiction. *Physiol Rev* **99**, 2115–2140 (2019).

71. Miller, E. K. & Cohen, J. D. AN INTEGRATIVE THEORY OF PREFRONTAL CORTEX FUNCTION. *Annu. Rev. Neurosci* **24**, 167–202 (2001).